Two epochs of eclogite metamorphism link 'cold' oceanic subduction and 'hot' continental subduction, the North Qaidam UHP belt, NW China

SHUGUANG SONG[1]*, YAOLING NIU[2,3], GUIBIN ZHANG[1] & LIFEI ZHANG[1]

[1]*MOE Key Laboratory of Orogenic Belts and Crustal Evolution, School of Earth and Space Sciences, Peking University, Beijing 100871, China*

[2]*Department of Earth Sciences, Durham University, Durham DH1 3LE, UK*

[3]*Institute of Oceanology, Chinese Academy of Science, Qingdao 266071, China*

S.S., 0000-0002-0595-7691

**Correspondence:* *sgsong@pku.edu.cn*

Abstract: Eclogites in the high-pressure (HP) and ultrahigh-pressure (UHP) belts record subduction-zone processes; exhumed eclogites of seafloor protoliths record low-temperature (mostly <600°C), high-pressure and 'wet' environments: that is, relatively 'cold' subduction with highly hydrous minerals such as lawsonite. In contrast, eclogites formed by the continental subduction record relatively 'hot' ($T > 650$°C) and 'dry' ultrahigh-pressure metamorphic (UHPM) conditions with syncollisional magmatism. Here, we investigate some eclogites from two ophiolite sequences that intercalated in the North Qaidam UHPM belt, which is genetically associated with continental subduction/collision. The observations of lawsonite pseudomorphs in garnets, garnet compositional zoning, mineral and fluid inclusions in zircons, and zircons with distinct trace-element patterns and U–Pb ages all suggest that these eclogites represent two exhumation episodes of subduction-zone metamorphic rocks: the early 'cold' and 'wet' lawsonite eclogite and the late 'hot' and 'dry' UHP kyanite eclogite. The early lawsonite-bearing eclogite gives metamorphic ages of 470–445 Ma and the later kysnite-bearing eclogite gives metamorphic ages of 438–420 Ma, with a time gap of *c.* 7–10 myr. This gap may represent the timescale for transition from oceanic subduction and continental subduction to depths greater than 100 km. We conclude that evolution from oceanic subduction to continental collision and subduction was a continuous process.

In addition, we find that titanium contents in zircons have a positive correlation with U contents. Ti-in-zircon thermometry is likely to be invalid or limited for low-temperature eclogites.

Supplementary material: Mineral composition data from the field sites are available at https://doi.org/10.6084/m9.figshare.c.4024774.v1

Eclogite, as an important rock type within orogenic belts, records processes of subduction and exhumation of both oceanic and continental lithospheric materials. They usually occur in two individual end-member subduction zones (i.e. the oceanic-type and continental-type) within the continental orogenic belts.

Oceanic subduction and continental subduction zones are distinctive in rock assemblage and their detailed dynamics of subduction processes are only poorly known (Maruyama *et al.* 1996; Ernst 2001; Song *et al.* 2006, 2014*a*; Rubatto *et al.* 2011). The relationship between the oceanic subduction (usually cold and negative buoyancy) and continental subduction (usually hot and buoyancy) is also an issue of ambiguity. As a consensus, continental crust is less dense than that of the oceanic counterpart, and less likely to sink into the mantle (e.g. Brueckner 2011). Therefore, a pull force from previously subducted oceanic lithosphere plays an important role in dragging the continental lithosphere to depths greater than 100 km (e.g. Chemenda *et al.* 1996; Ernst 2005; Brueckner 2006).

Most high-pressure (HP) and ultrahigh-pressure (UHP) metamorphic zones record a complex process of subduction and exhumation: for example, two cycles of yo-yo subduction and exhumation would occur within less than 20 myr (Rubatto *et al.* 2011), and two orogenic cycles were recorded in one eclogite sample (Herwartz *et al.* 2011). The transition from oceanic subduction to continental collision and subduction, on the other hand, is a more complex process and two aspects remain to be particularly figured out: (1) the influence on the

From: Zhang, L. F., Zhang, Z., Schertl, H.-P. & Wei, C. (eds) *HP–UHP Metamorphism and Tectonic Evolution of Orogenic Belts*. Geological Society, London, Special Publications, **474**, https://doi.org/10.1144/SP474.2

former subducted oceanic slab during the continental zcollision/subduction; and (2) the timescale for the transition from oceanic subduction to continental subduction and exhumation. The presence of UHP metamorphic ophiolite sequences within the continental subduction zones (e.g. Song *et al.* 2006, 2009; Zhang *et al.* 2008) provide opportunities to reveal the two cycles of eclogite-facies metamorphism and the transition of oceanic–continental subduction.

Two kinds of eclogites have been identified in the broad Qilian Orogen: low-temperature (<600°C), lawsonite-bearing eclogites in the North Qilian accretionary belt (Song *et al.* 2007; Zhang *et al.* 2007); and high-temperature eclogite ($T > 650$°C) in the North Qaidam ultrahigh-pressure metamorphic (UHPM) belt (e.g. Song *et al.* 2014*b* and references therein). They represent cold oceanic subduction and hot continental collision/subduction, respectively. In this paper, we report two epochs of eclogite-facies metamorphism that recorded early lawsonite eclogite to late kyanite eclogite in some individual samples from the North Qaidam UHP metamorphic belt, which confirm a complete process from 'cold' oceanic subduction to 'hot' continental subduction. This process will help us in understanding the dynamic process of connection between the oceanic subduction and the subsequent continental subductions.

Geological setting

Two kinds of subduction belts (i.e. the North Qilian oceanic 'cold' subduction zone in the north and the North Qaidam continental subduction belt in the south) extend parallel in the northern Qinghai–Tibet Plateau. The North Qilian orogenic belt in the north is the type oceanic suture zone and contains early Paleozoic ophiolite sequences, HP metamorphic belts, island-arc volcanic rocks and granitic plutons, Silurian flysch formations, Devonian molasse, and Carboniferous–Triassic sedimentary cover sequences (see Song *et al.* 2013 and references therein). Lawsonite in eclogite and Mg-carpholite in metapelite provide convincing evidence that the North Qilian HP metamorphic belt records cold oceanic lithosphere and a low geothermal gradient (6–7°C km^{-1}) in the early Paleozoic (Song *et al.* 2007; Zhang *et al.* 2007).

The North Qaidam UHPM belt in the south is located in the north margin of the Qaidam Basin, between the Qilian Block and Qaidam Block, and extends for about 400 km (see Fig. 1). The North Qaidam UHPM belt consists mainly of granitic and pelitic gneisses intercalated with blocks of eclogite, and varying amounts of ultramafic rocks, especially garnet peridotite. The rock assemblages suggest that this belt is typical of a continental-type subduction zone (Song *et al.* 2014*b* and references therein), different from the 'cold', oceanic-type subduction of the North Qilian Suture Zone.

Coesite inclusions have been identified in zircon and garnet from metapelite and eclogite at Dulan, Xitieshan and Yuka (Yang *et al.* 2002; Song *et al.* 2003*a*, *b*, 2006; Zhang *et al.* 2009; Zhang *et al.* 2010; Liu *et al.* 2012), and diamond in zircon from the garnet peridotite at Lüliangshan (Song *et al.* 2005), respectively. Pressure and temperature (*P–T*) estimates of the enclosing eclogite and garnet peridotite establish the North Qaidam eclogite belt as an Early Paleozoic UHPM terrane exhumed from depths of 100–200 km.

Two rock types of eclogitic protoliths have been identified in the North Qaidam UHPM belt: (1) the 850–820 Ma continental flood basalts (CFBs) with a mantle-plume origin (Chen *et al.* 2009; Song *et al.* 2010; Zhang *et al.* 2010; Xu *et al.* 2016); and (2) 540–500 Ma ophiolite with UHPM harzburgite, cumulate gabbro (kyanite eclogite) and N- to E-type basalts (Song *et al.* 2006, 2009; Zhang *et al.* 2008). It is notable that all eclogites from the 850–820 Ma CFBs have only one epoch of UHP metamorphism at 440–430 Ma (Chen *et al.* 2009; Song *et al.* 2010; Zhang *et al.* 2010).

Sample petrography

Two types of eclogite samples from two sections in the well-studied Dulan UHP terrane were carefully investigated (see the localities in Fig. 1a). One is the bimineral eclogite with protoliths of low-K tholeiitic basalt (Song *et al.* 2006); the other is kyanite eclogite from cumulate gabbro in a UHP metamorphic ophiolite sequence (e.g. Zhang *et al.* 2008).

Basaltic bimineral eclogite in the Yematan section

Samples was collected from a large massive eclogite block (200 × 800 m in size) in the Yematan section; this cross-section exposes blocks of garnet-bearing, strongly garnet-bearing serpentinized peridotite (Mattinson *et al.* 2006), garnet-bearing pyroxenite and eclogite intercalated with coesite-bearing metapelite (Yang *et al.* 2002; Song *et al.* 2003*a*, *b*, 2006, 2009), and 950–910 Ma granitic gneisses (Song *et al.* 2012) (Fig. 1b). The garnet pyroxenite was interpreted to be an ultramafic cumulate and the eclogite blocks are geochemically similar to present-day N-type to E-type mid-ocean ridge basalt (MORB) (Song *et al.* 2003*b*, 2006). This rock assemblage resembles a dismembered ophiolite (Song *et al.* 2009) with protolith ages of *c.* 500 Ma (Han 2015).

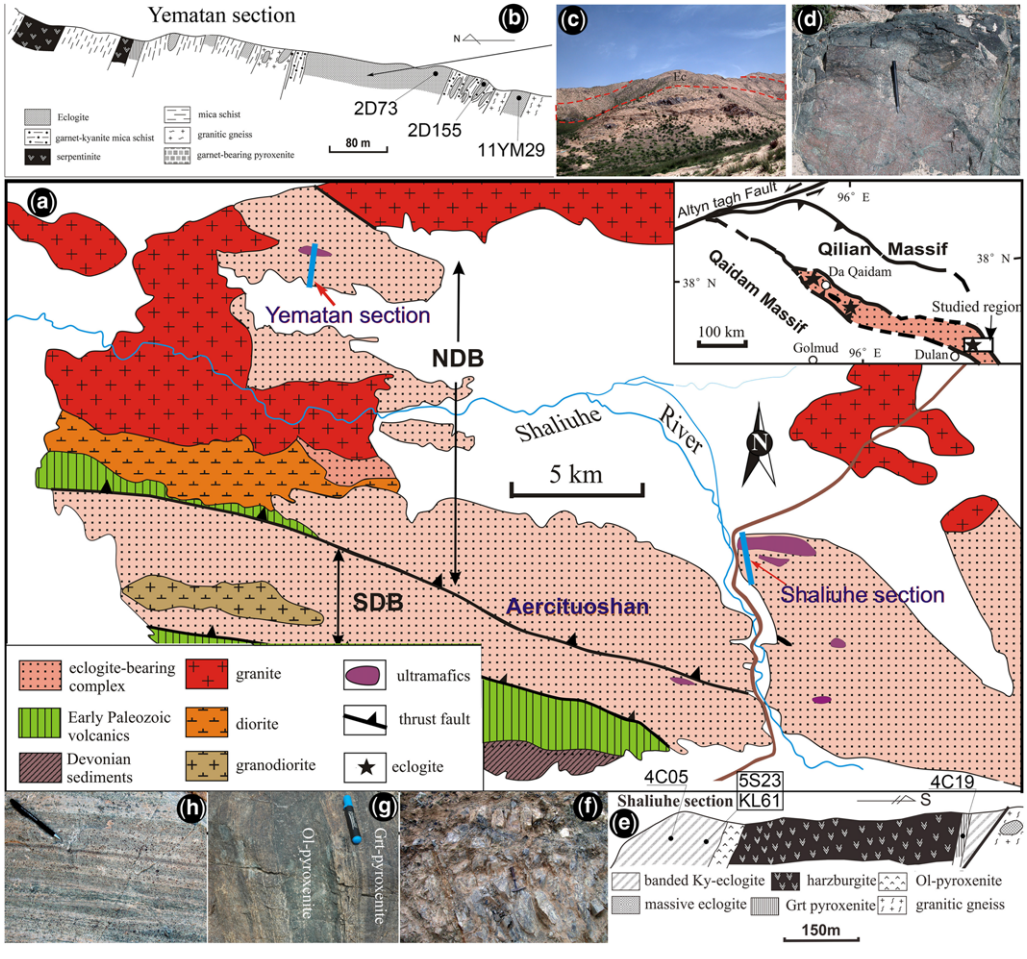

Fig. 1. (**a**) Geological map of the Dulan UHPM terrane with two ophiolitic sections (after Song *et al.* 2003*a*, *b*). The Yematian section (**b**) consists of UHP metamorphosed serpentinite, garnet pyroxenite, gabbroic and basaltic eclogites (**c**) & (**d**). The Shaliuhe section (**e**) consists of UHP metamorphosed harzburgite (**f**), garnet pyroxenite and olivine pyroxenite (**g**), and kyanite eclogite (cumulate gabbro) (**h**).

The studied eclogite samples (2D73, 2D155 and 11YM29) were very fresh, show a granoblastic texture without being deformed, and consist of garnet (*c.* 35%), omphacite (*c.* 60%) and rutile (*c.* 1–2%), with very rare phengite and the least amphibole overprinting (Fig. 2a). The protolith is low-K basalt in composition and exhibits geochemical characters of normal-type MORB (N-MORB) affinity (Song *et al.* 2006). We named it basaltic eclogite. In this eclogite, omphacite is equigranular, relatively small in size and chemically homogeneous; garnet occurs as porphyroblasts uniformly distributed in the matrix of omphacite (Fig. 2a). The peak metamorphic conditions of bimineral eclogites are at $T = 650–700°C$ and $P = 2.8–3.3$ GPa (Song *et al.* 2003*a*, *b*; Zhang *et al.* 2010); some are overprinted by granulite-facies metamorphism and partial melting at $T = 870–950°C$ and $P = 1.9–2.0$ GPa (Song *et al.* 2003*b*, 2014*a*).

Gabbroic kyanite eclogite in the Shaliuhe ophiolite sequence

The gabbroic eclogite (including samples KL61, 4C05 and 4C19) was collected from the well-studied Shaliuhe UHPM ophiolite section, which contains (1) serpentinized harzburgite; (2) garnet-bearing pyroxenite and olivine pyroxenite; (3) kyanite eclogite; and (4) massive eclogite (Fig. 1e–h). The peridotite block is dark-coloured, strongly serpentinized, and is apparently conformable with pyroxenites and kyanite eclogite. Relict olivine and orthopyroxene (opx) with two types of olivine (relict olivine from

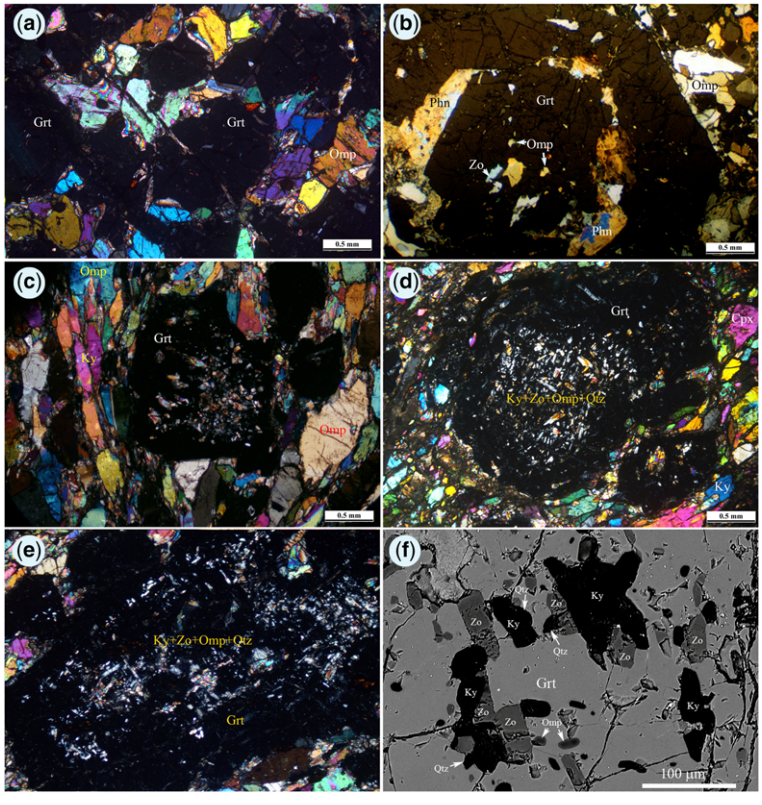

Fig. 2. Photomicrographs showing textures of the two types of eclogites. (**a**) Granoblastic texture of the basaltic bimineral eclogite (2D73) in the Yematan section. (**b**) Garnet (Grt) porphyroblast shows two stages of growth. The core domain is rich in mineral inclusions of zoisite (Zo) + omphacite (Omp), and phengite (Phn) occurs around the first stage of garnet. (**c**) Ky-eclogite (4C05) with the mineral assemblage Grt + Omp + Ky + Rt. Garnet has a large number of mineral inclusions of Zo + Ky + Omp + Qtz in the core domain. (**d**) & (**e**) Porphyritic garnet with mineral inclusions of Zo + Ky + Omp + Qtz from Ky-eclogite samples 5C23 and 6KL61, respectively. (**f**) Mineral inclusions kyanite (Ky), zoisite (Zo), omphacite(Omp) and quartz (Qtz) in garnet. The assemblage Ky + Zo + Qtz is most likely to be the product of lawsonite decomposition.

the oceanic mantle and metamorphic olivine during UHP metamorphism) have been identified in the serpentinized peridodite (Zhang *et al.* 2008; Song *et al.* 2009). Both the garnet-bearing pyroxenite and kyanite eclogite retain a banded structure that has been confirmed as inherited from original ultramafic and gabbroic cumulates (Fig. 1g, h). Geochemical analyses further indicate that this banded kyanite eclogite has characteristics of cumulate gabbro, with large amounts of Al_2O_3 (17.2–22.7 wt%), CaO (12.5–13.5 wt%), MgO (7.2–13.5 wt%), Cr (422–790 ppm), Ni and Sr, and low TiO_2 and REE, and shows strong positive Eu anomalies (Eu* 1.51–2.08) (Zhang *et al.* 2008). We therefore named it gabbroic Ky-eclogite (Table 1).

The Ky-eclogite has the mineral assemblage of garnet (Grt), omphacite (Omp), kyanite (Ky) and rutile (Rt), with retrograde overprinting by amphibole. Phengite (Phn) is a minor phase that occasionally occurs in matrix or as inclusion in omphacite and garnet, and no epidote (Ep) or zoisite (Zo) was found in the matrix. The Grt–Omp–Phn–Ky geothermoborameter of Ravna & Terry (2004) yielded peak *P–T* conditions of $P = 2.7$–3.4 GPa and $T = 630$–770°C (Song *et al.* 2003*a*, *b*; Zhang *et al.* 2008).

Mineral abbreviations are after Whitney & Evans (2010).

Analytical methods

Mineral analyses were performed on a JEOL JXA-8100 Electron Probe Microanalyzer (EPMA) at Peking University. Analytical conditions were optimized for standard silicates and oxides at

Table 1. *Mineral composition of gabbroic Ky-eclogite*

Sample mineral	KL61-1.1 Omp-in	KL61-1.2 Omp-in	KL61-1.3 Omp-in	KL61-2.1 Omp	KL61-2.2 Omp	KL61-2.3 Omp	KL61-1 Zo-in	KL61-2 Zo-in	KL61-3 Zo-in
SiO_2	54.71	54.49	54.2	55.78	55.17	55.65	39.69	39.10	39.02
TiO_2	0.05	0.08	0.03	0.13	0.13	0.05	0.11	0.05	0.07
Al_2O_3	7.57	8.23	7.82	8.54	9.45	9.12	33.62	33.58	33.22
Cr_2O_3	0	0.03	0.11	0.03	0.66	0.11	0.01	0.06	0.08
FeO	2.22	2.36	2.35	2.15	1.81	1.85	0.92	1.50	0.98
MnO	0.05	0.06	0.03	0.05	0.02	0	0.01	0.04	0.07
NiO	0	0.01	0.05	0.03	0.02	0.03	0.00	0.00	0.00
MgO	12.17	12.2	12.44	12.02	10.86	12.01	0.01	0.09	0.12
CaO	18.28	17.74	18.25	16.56	16.81	16.82	23.69	23.26	23.90
Na_2O	4.55	5.09	4.67	4.54	4.26	4.22	0.01	0.00	0.02
K_2O	0.01	0.01	0.02	0	0.02	0	0.00	0.00	0.02
Total	99.61	100.3	99.97	99.83	99.21	99.86	98.07	97.68	97.50
O	6	6	6	6	6	6	12.5	12.5	12.5
Si	1.952	1.922	1.923	1.987	1.989	1.984	3.004	2.979	2.980
Ti	0.001	0.002	0.001	0.003	0.004	0.001	0.006	0.003	0.004
Al	0.318	0.342	0.327	0.359	0.401	0.383	2.998	3.015	2.990
Cr	0.000	0.001	0.003	0.001	0.019	0.003	0.001	0.004	0.004
Fe^{3+}	0.066	0.070	0.070	0.000	0.000	0.000	0.039	0.064	0.042
Fe^{2+}	0.000	0.000	0.000	0.064	0.055	0.055			
Mn	0.002	0.002	0.001	0.002	0.001	0.000	0.000	0.001	0.002
Ni	0.000	0.000	0.001	0.001	0.001	0.001	0.000	0.000	0.000
Mg	0.647	0.642	0.658	0.638	0.584	0.638	0.001	0.005	0.007
Ca	0.699	0.671	0.694	0.632	0.649	0.642	0.960	0.949	0.978
Na	0.315	0.348	0.321	0.314	0.298	0.292	0.000	0.000	0.001
K	0.000	0.000	0.001	0.000	0.001	0.000	0.000	0.000	0.000
Sum	4	4	4	4	4	4	7.009	7.020	7.008
Jd	27.13	26.67	25.09	34.89	39.39	36.85			
Ae	6.62	6.96	7.00	0	0	0			
Fe/(Fe + Al)							0.013	0.021	0.014

Fe^{3+} is calculated after Droop (1987).
in, inclusion.

15 kV accelerating voltage with a 20 nA focused beam current for all the elements. Routine analyses were obtained by counting for 30 s at peak and 10 s on background. Repeated analysis of natural and synthetic mineral standards yielded precisions better than ±2% for most elements.

Zircon grains from the Shaliuhe gabbroic Ky-eclogite (5S23: Zhang *et al.* 2008; 2D19 and 4C04) and Yematan basaltic eclogite were studied for their cathodoluminescent (CL) images, mineral inclusions and U–Pb isotopic dating. The internal zoning was examined using a CL spectrometer (Garton Mono CL3+) equipped on a Quanta 200F ESEM with 2 min scanning time at conditions of 15 kV and 120 nA at Peking University. Zircons were analysed for U, Pb and Th isotopes using SHRIMP II at the Beijing SHRIMP Centre, Chinese Academy of Geosciences. Instrumental conditions and measurement procedures follow Compston *et al.* (1992). The spot size of the ion beam was about 25 μm in diameter, and the data were collected in sets of five scans through the masses with 2 nA primary O_2^- beams. The reference zircon was analysed first, and again after every three unknowns. The measured $^{206}Pb/^{238}U$ ratios in the samples were corrected using reference zircon standard SL13 from a pegmatite from Sri Lanka ($^{206}Pb/^{238}U = 0.0928$; 572 Ma) and zircon standard TEMORA (417 Ma) from Australia (Black *et al.* 2003). The common-Pb correction used the $^{206}Pb/^{204}Pb$ ratio and assumed a two-stage evolution model (Stacey & Kramers 1975). Concordia ages and diagrams were obtained using Isoplot/Ex (3.0) and the mean ages are weighted means at 95% confidence levels (Ludwig 2003).

Measurements of U, Th, Pb and trace elements in zircons were conducted on laser ablation-inductively coupled plasma-mass spectrometry (LA-ICP-MS) at the Chinese University of Geoscience and Peking University. A laser spot size of 32–36 μm, a laser energy density of 8.5 J cm^{-2} and a repetition rate of 10 Hz were applied for analysis. Detailed analytical procedures are similar to those described by Song *et al.* (2010). Calibrations for elemental

concentration were carried out using NIST 610 glass as an external standard, with recommended values taken from Pearce *et al.* (1997) and using ^{29}Si as an internal standard. NIST 612 and 614 served as monitoring standards at the same time. The analytical accuracy for titanium in zircon is better than ±5% with abundances >100 ppm, and about ±10% with abundances <10 ppm.

Two epochs of eclogite metamorphism recorded in garnet

All garnet porphyroblasts in the gabbroic kyanite eclogite and basaltic bimineral eclogite show a clear core–rim structure; they are defined both by mineral inclusions and chemical patterns, and exhibit clear two-stage overgrowth (Fig. 2b). In the kyanite eclogite (KL61), the core domain of garnet contains abundant mineral inclusions, but the rim domain is fairly clean (Fig. 2c). This core–rim structure is a common feature for garnet in all low-temperature (especially lawsonite-bearing) eclogites (e.g. Clarke *et al.* 1997; Song *et al.* 2007), but less common in the high-temperature eclogites in the continental-type UHPM belt.

Lawsonite pseudomorph in garnet from the Ky-eclogite

Mineral inclusions in the core domain of garnets from the Ky-eclogite (samples 4C04, 5S23 and KL61) are kyanite, zoisite, omphacite and quartz. They show rectangular and triangular shapes (Fig. 2d). Zoisite inclusions are characterized by extremely low pistacite (Ps) in composition (Ps = 100 × Fe^{3+}/ (Fe^{3+} + Al) = 1.1–2.1 mol%) (see the Supplementary material). This mineral assemblage is most likely to comprise lawsonite psedomorphs and define a possible reaction of the form:

$4CaAl_2[Si_2O_7](OH)_2(H_2O) = 2Ca_2Al_3(Si_2O_7)(SiO_4)O(OH) + Al_2SiO_5 + SiO_2 + 7H_2O$ (i.e. Lws = Zo + Ky + Qtz + H_2O). Unlike the retrograde process (e.g. Whitney & Davis 2006), progressive metamorphism can also exceed the stability field of the lawsonite, which destroys the lawsonite eclogite.

Omp inclusions in garnet have a slightly higher molar proportion (mol%) of aegrine (Ae = 6.1–7.0 mol%) and lower jadeite (Jd = 25–27 mol%) than Omp in the matrix (Ae = 0, Jd = 35–39 mol%), suggesting a lower-temperature condition in the core domain.

The numerous lawsonite pseudomorphs in garnet suggest that lawsonite was ubiquitous during the first epoch of lawsonite eclogite-facies metamorphism associated with cold and water-saturated oceanic subduction.

Garnet compositional profiles

Garnet from the gabboic Ky-eclogite has much higher MgO and CaO contents than from the basaltic eclogite. A porphyroblast garnet from the gabbroic eclogite was chosen for compositional profile analyses. As shown in Figure 3a, two epochs of progressive growth zonation are recognized in the profile (see the Supplementary material); in the core domain, grossular decreases smoothly from the centre (Grs 23.33 mol%) to the core–rim boundary (Grs 21.1 mol%), almandine falls from 35.65 to 34.91, whereas pyrope increases from 40.37 to 43.01 mol%. Chemical zoning sharply changes in the core–rim boundary: grossular bounds up to 23.87 mol%, almandine to 36.94 mol% and pyrope drops down to 39.3 mol%.

Some garnet porphyroblasts in sample 2D73 also exhibit a core–rim structure; zoisite, amphibole and omphacite occur in the core, and phengite inclusions occur at the core–rim boundary (Fig. 2b). No lawsonite or its pseudomorph was observed. Compositional zoning shows similar pattern with a

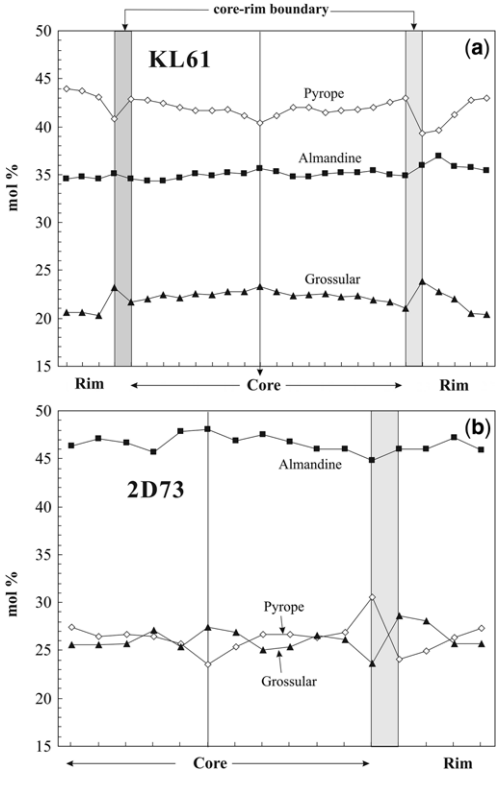

Fig. 3. Composition profiles of garnets from a kyanite eclogite (KL61) and bimineral basaltic eclogite 2D73.

sharp change at the core–rim boundary (Fig. 3b) (see the Supplementary material).

The sharp increase in glossular at the core–rim boundaries can be explained by the decomposition of lawsonite with an increase in pressure and temperature, which can release large amounts of glossular composition into garnet at UHP conditions beyond the lawsonite stability field. Dehydration of lawsonite during continental subduction will give rise to exhumation and decompression melting of the subducted oceanic slab (Song *et al.* 2014*b*).

P–T *estimate for the Ky-eclogite*

Petrographical observations indicate that eclogite-facies metamorphic epoch recorded in the core domain of garnet contains a low-temperature assemblage Grt + Omp + Lws ± Phn + Qtz/Coe + Rt, as lawsonite presents as psudomorphs of Ky + Zo + Qtz. Using compositions of clinopyroxene (Cpx) inclusions in garnet and the surrounding garnet, and assuming the presence of Phn, and using the geothermobarometry of Ravna & Terry (2004), we obtained the *P–T* conditions for the first epoch of eclogite metamorphism at $T = 547–603°C$ and $P = 2.6–2.7$ GPa, which are well within the lawsonite stability field.

Using the rim composition of garnet and omphacite in the matrix, the assemblage Grt + Omp + Ky + Phn in the matrix gave $P = 3.2–3.3$ GPa and $T = 698–721°C$, while Fe^{3+} in omphacite was assumed $Fe^{3+} = (Na–Al–Cr)$.

Two epochs of eclogite metamorphism recorded by zircons

Zircons from six represented, well-studied eclogite samples were re-examined for inner structures (CL), mineral inclusions and ages, and zircon REE patterns. These samples include basaltic bimineral eclogite from the Yematian ophiolite section (2D73, 2D155 and 11YM29), and Ky-eclogite and Grt-pyroxenite from the Shaliuhe ophiolite section (4C05, 4C19 and 5S23), respectively.

Zircon structure and mineral/fluid inclusions

All three eclogite samples (2D73, 2D155 and 11YM29) from the Yematan ophiolitic sections were all fresh with the least retrograde mineral (Amp) overprinting (Fig. 2a, b). However, almost all zircons from these samples exhibit a core–rim structure in CL images; the core domains show dark luminescence emission (fluid-rich and high U, Th contents) and fir-tree sector zones; and the rim shows intermediate luminescence emission (Fig. 4). Besides Grt, Omp and Rt inclusions, Qtz and a large quantity of water-dominant fluid inclusions were also identified using Raman spectrum in the core domain (Fig. 4a, b), which suggests that the zircon cores were crystallized in a water-rich and quartz-stability condition. As shown in Figure 4c, eclogite-facies mineral inclusions Grt, Omp and Rt are found in both core and rim domains.

CL images suggest that zircons from the gabbroic Ky-eclogite also have two distinct stages of growth with a core–rim structure. In sample 5S23, some grains retain a magmatic core with oscillatory zones, representing relicts from its protolith of cumulate gabbro, and have, therefore, determined the formation age of the ophiolite at 517 ± 11 Ma (Zhang *et al.* 2008). The texturally old core shows dark luminescence emission and weak zoning. The texturally young zircon rim show strong/intimidate luminescence (Fig. 4c, d), and occurs either as rims around old core or as single crystals. Mineral inclusions of garnet, omphacite and rutile are also observed in both core and rim domains.

Two epochs of metamorphic ages

Table 2 lists the published results of SHRIMP (sensitive high-resolution ion microprobe) dating for eclogites from UHP metamorphic ophiolitic sequences in the Dulan UHPM terrane. Zircons from the basaltic eclogite 2D155 in the Yematan have large, dark luminescence cores and narrow, intermediate luminescence rims. No magmatic relict core was observed. Fourteen cores gave a weighted $^{206}Pb/^{238}U$ mean age of 457 ± 7 Ma (MSWD = 0.91) and one rim gave an apparent age of 426 ± 12 Ma (Song *et al.* 2006). For basaltic eclogite 2D73, two zircon grains contained relict magmatic cores, and yielded $^{206}Pb/^{238}U$ apparent ages of 485 ± 24 and 481 ± 24 Ma, which should represent the protolith age of the ophiolite sequence. Eight metamorphic cores analysed by SHRIMP formed a weighted $^{206}Pb/^{238}U$ mean of 462 ± 13 Ma (MSWD = 0.41), and 14 analyses for rims and weak luminescent grains gave a weighted mean age of 424 ± 13 Ma (MSWD = 0.12). For basaltic eclogite sample 11YM 29, 17 cores gave a weighted mean age of 448 ± 6 Ma (MSWD = 4.4), and nine rims gave a weighted mean age of 425 ± 6 Ma (MSWD = 1.2) (Zhang *et al.* 2014).

In the gabbroic sample (5S23) from the Shaliuhe UHP metamorphic ophiolite sequence, magmatic zircon relicts with oscillatory zoning gave a weighted mean age of 516 ± 8 Ma (MSWD = 1.9) (Zhang *et al.* 2008), suggesting that the oceanic crust formed in the late Cambrian, similar to ophiolites in the North Qilian Suture Zone (Song *et al.* 2013). Eleven metamorphic cores formed a weighted

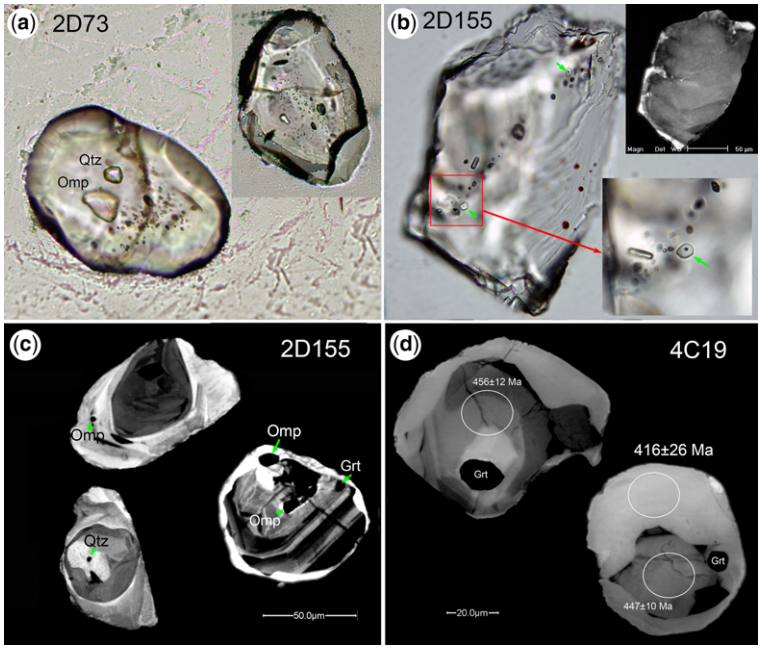

Fig. 4. Representative photomicrographs of zircons and their CL images. (**a**) omphacite (Omp), quartz and small fluid inclusions in zircon cores (2D73). (**b**) Banded fluid inclusions in a zircon grain (2D155). These water-rich fluid inclusions show oval, tubular and negative crystal shapes. The two negative crystal inclusions (arrow) show a major liquid phase with a small vapour bubble. (**c**) Zircon CL images showing an obverse core–rim structure. The core domain contains Grt, Omp and Qtz inclusions, whereas the rim domain also has Omp inclusions. (**d**) Zircon CL images showing the core–mantle structure with garnet inclusions and ages.

mean age of 450 ± 7 Ma, and 13 rims and weak luminescent grains give a mean of 426 ± 13 Ma. Sample 4C05 is also a Ky-eclogite from the Shaliuhe section. One zircon core gave a $^{206}Pb/^{238}U$ age of 468 ± 16 Ma, and 13 grains with intermediate luminescence emission yielded a weighted mean age of 425 ± 8 Ma.

Sample 4C19 is a garnet-pyroxenite metamorphosed from a high-Mg cumulate in the Shaliuhe ophiolite sequence. Six analyses for dark luminescence cores yielded weighted mean ages of 450 ± 7 Ma (MSWD = 0.31), and nine analyses for rims and weak luminescent grains gave a weighted mean age of 425 ± 9 Ma (MSWD = 0.50).

Table 2. *Zircon U–Pb SHRIMP ages of eclogites from the Yematan ophiolitic section and Shaliuhe ophiolitic section*

Sample	Rock type	Protolith age	Stage I (core) (Lws-eclogite)	Stage II (rim) Ky-/Zo-eclogite	References
2D155	Basaltic eclogite (Yematan)	No magmatic core	457 ± 7 Ma n = 15	426 ± 12 Ma n = 1	Song *et al.* (2006); this study
2D73	Basaltic eclogite (Yematan)	485 ± 23 Ma	452 ± 15 Ma n = 10	424 ± 13 Ma n = 14	Song *et al.* (2014*a*); this study
11YM29	Basaltic eclogite (Yematan)	No magmatic core	448 ± 6 Ma n = 17	425 ± 6 Ma n = 9	Zhang *et al.* (2014)
5S23	Gabbroic Ky-eclogite (Shaliuhe ophiolite)	516 ± 8 Ma n = 7	450 ± 7 Ma n = 11	426 ± 13 Ma n = 13	Zhang *et al.* (2008)
4C05	Gabbroic Ky-eclogite (Shaliuhe ophiolite)	No magmatic core	468 ± 16 Ma n = 1	425 ± 8 Ma n = 13	Song *et al.* (2014*a*)
4C19	Grt-pyroxenite (Shaliuhe ophiolite)	No magmatic core	450 ± 11 Ma n = 6	425 ± 9 Ma n = 9	Song *et al.* (2014*a*)

Zircon uranium contents and REE patterns

As a fluid-mobile element, it is expected that uranium (U) can enrich in zircon in a water-dominated fluid-rich environment. The U concentration of metamorphic zircons depends on the decomposition of the U-containing, fluid-rich minerals. Figure 5 summarizes the U contents of all zircons from the eclogite samples (Table 1) (see also the Supplementary material). The magmatic relict zircon cores of the gabbroic Ky-eclogite have a high and relatively uniform uranium content of 201–344 ppm (Fig. 5). The old metamorphic cores contain variable, but remarkably higher, uranium content (40–800 ppm, mostly >60 ppm) than the young metamorphic rims (7–141 ppm, mostly <50 ppm), suggesting that the core domain grew in a relatively wet, water-rich environment, whereas the rim domain grew in a relatively dry condition.

Zircons from basaltic eclogite samples 2D73, 11YM29 and 2D155 were analysed for trace elements, and zircon from one lawsonite eclogite sample (QS45) in the North Qilian Suture Zone was also analysed for comparison (Fig. 6).

Zircons from the lawsonite eclogite (QS45) show dark luminescence with heterogeneous growth textures of 'fir-tree' or radial sector zoning in the CL image (Fig. 6a). Some zircon core parts are rich in heavy-REE (HREE) and show obvious negative Eu* anomalies (0.28–0.39), suggesting that they might grow a little earlier than garnet; whereas the rim parts contains relatively lower HREE than the core parts and show no Eu* anomaly. All of these zircons show a steep HREE-enriched pattern with high contents of Yb and low contents of $[Tb/Yb]_N$ (0.05–0.24), which, together with their high U, suggests that they should be grown together with lawsonite at a fluid-rich environment.

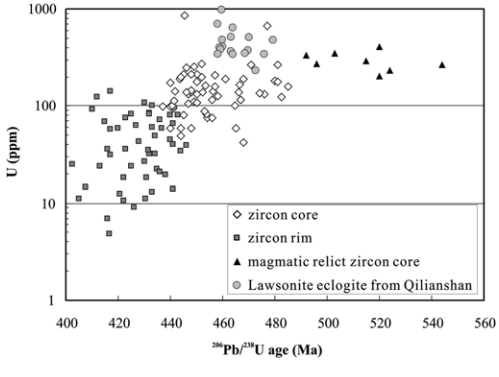

Fig. 5. Diagram for uranium v. $^{206}Pb/^{238}U$ age of magmatic relicts, and metamorphic zircon cores and rims (samples are listed in Table 1). The magmatic relict cores are from the gabbroic eclogite sample (5S23: Zhang *et al.* 2008). Zircons of the lawsonite-bearing eclogites are from the North Qilian Suture Zone (Song *et al.* 2004, 2006; Zhang *et al.* 2007).

Three metamorphic zircon inner cores of sample 2D73 show similar REE patterns with, but have a weaker Eu* anomaly (0.65–0.90) than, zircon cores of the Qilian lawsonite eclogite. Other cores show weakly enriched HREE patterns, and three zircons have extremely high-REE (LREE), suggesting strong fluid activity. All rims (or whole grains with a strong CL luminescent image) have low contents of REE and show flat or depleted HREE patterns with chondrite-normalized $[Tb]_N/[Yb]_N$ mostly >1 (Fig. 6b).

Zircon cores of 11YM29 exhibit a large variety of REE patterns, changing gradually from steep HREE pattern to flat HREE patterns (Fig. 6c). This variation is most probably in equilibrium with garnet, from less to more of a garnet presence during zircon growth. All of them have no significant Eu anomaly, indicating the absence of coexisting plagioclase, and thus zircon growth is at high pressure beyond the stability of feldspar (Rubatto *et al.* 2011). The zircon rims show a depletion in HREE patterns with $[Tb]_N/[Yb]_N < 1$, suggesting that the supply of HREEs decreases when growing.

Zircons from 2D155 have a large core with dark luminescence and a fir-tree structure, and a thin bright rim. U–Pb analyses using LA-ICP-MS gave a mean $^{206}Pb/^{238}U$ age of 459.5 ± 4 Ma (MSWD = 0.59), the same as by the SHRIMP dating method (457 ± 7 Ma). Trace-element analyses show that zircons have rather uniform, weakly enriched HREE patterns ($[Tb]_N/[Yb]_N < 1$) and no Eu anomaly (Fig. 6d), similar to those metamorphic zircon cores described above.

Figure 7 shows a decrease in normalized HREE ($[Yb]_N$) with U–Pb ages from zircon core to rim. Zircon cores, which represent the first epoch of eclogite metamorphism, have much higher HREE values than rims, the second epoch of the eclogite metamorphism. With regard to the steep HREE pattern of the zircon cores, it was generally thought that garnet, which readily sequesters HREEs, was not a major constituent of the assemblage; in other words, zircon would grow earlier than garnet. However, garnet and omphacite inclusions in zircon cores suggest that they must grow concurrently during eclogite-facies metamorphism. Therefore, we suggest that water-rich fluids help HREEs to enter zircon, as opposed to garnet; the high uranium content in zircon cores can testify to this explanation.

In summary, zircon U–Pb analyses show that the two epochs of HP–UHP metamorphism are distinct. The early HP stage, from 468 to 448 Ma, with high uranium contents can be interpreted to be a time of oceanic 'wet and cold' subduction, while the late stage, from 430 to 425 Ma, is a time of UHP

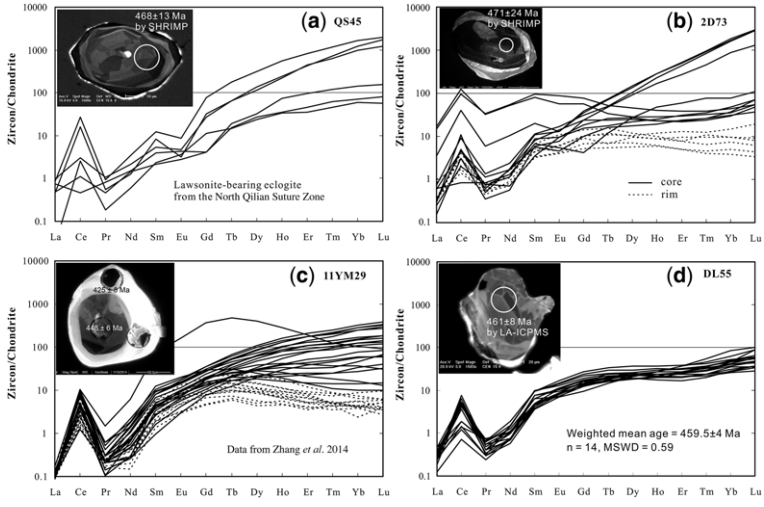

Fig. 6. Chondrite-normalized REE patterns for zircons from: (**a**) lawsonite eclogite (QS45) from the North Qilian Suture Zone with a mean age of 464 ± 6 Ma (Song *et al.* 2006); (**b**) & (**c**) basaltic eclogite with two stages of zircon growth from the North Qaidam UHPM belt; and (**d**) basaltic eclogite (2D155) with analyses of core domains in the North Qaidam UHPM belt.

metamorphism during continental subduction, as illustrated in Figure 8.

Discussion and conclusions

Two epochs of eclogite metamorphism at oceanic v. continental subduction

Seafloor subduction is generally cold (<550°C: e.g. Carswell 1990; Maruyama *et al.* 1996; Song *et al.* 2007; Agard *et al.* 2009), with abundant hydral minerals such as lawsonite, epidote/zoisite, glaucophene and carpholite (also see Xiao *et al.* 2012, 2013). The minerals, especially lawsonite and carpholite, contain a large amount of water, and can therefore introduce water into the deep mantle along the oceanic subduction channels to depths of greater than 100 km (e.g. Peacock & Wang 1999; Poli & Schemidt 2002).

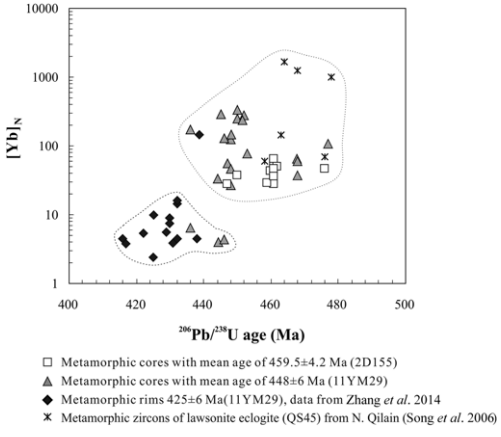

Fig. 7. Diagram of chondrite-normalized $[Yb]_N$ v. U–Pb ages of zircons from the core to the rim.

All studied eclogite samples came from ophiolitic sequences, the oceanic slab that was previously preserved before continental collision. All lines of evidence described above, including (1) lawsonite pseudomorphs in garnet and their variation in composition profiles, (2) the decrease in uranium content from zircon core to rim, and (3) the REE patterns and two distinct stages of ages in metamorphic zircons, afford that they have experienced two cycles of eclogite-facies metamorphism. The first epoch is 'cold and wet': lawsonite-eclogite facies at *P–T* conditions of 2.6–2.7 GPa and 547–603°C related to the oceanic subduction, similar to, or little higher than, the lawsonite eclogite in the North Qilian Suture Zone (e.g. Song *et al.* 2007; Zhang *et al.* 2007; Wei *et al.* 2009). The second epoch, on the other hand, is 'dry and hot': kyanite-eclogite facies at *P–T* conditions of 3.2–3.3 GPa and 700–720°C related to the continental subduction (Fig. 8). The garnet peridotites, felsic gneisses and eclogites with protoliths of 850–820 Ma CFBs have experienced this epoch of the UHP metamorphic event (see below).

We illustrate that the oceanic crust first subducted to mantle depth at 462–445 Ma, and exhumed to the shallow-crust level, then subducted to mantle depth again with UHP metamorphism at 438–420 Ma.

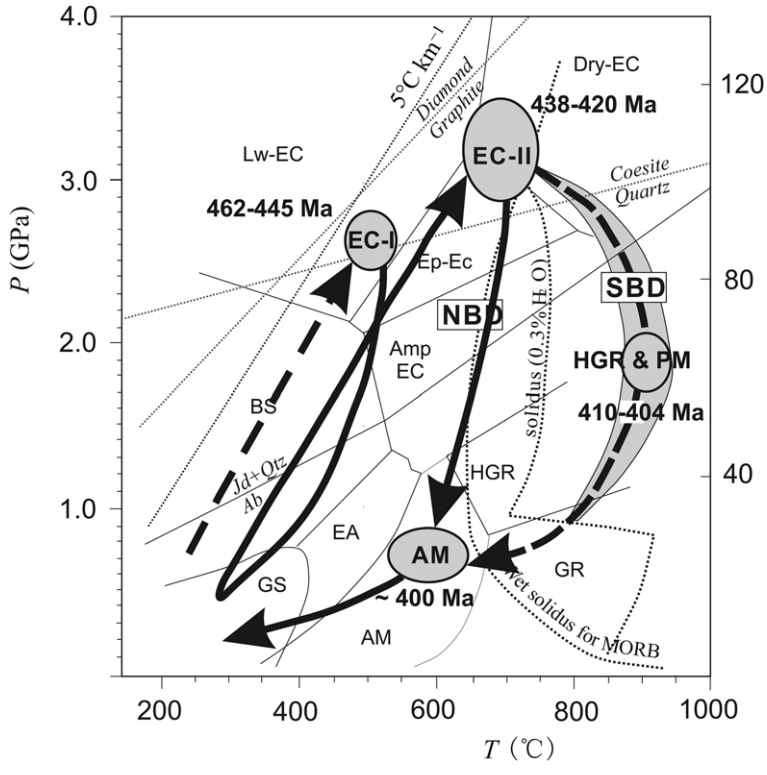

Fig. 8. The pressure–temperature–time (*P–T–t*) path of the North Qaidam UHP eclogites illustrates the process for the 'cold' ocean subduction to the 'hot' continental subduction. The path to high-pressure granulite (HGR) and partial melting (PM) is determined by Song *et al.* (2003*b*, 2014*a*).

Eclogites themselves cannot give evidence for this supposed process. However, the mantle peridotite, the basal part of the Shaliuhe ophiolite (Fig. 1), has experienced such a process: the first exhumation caused strong serpentinization, and then the serpentines were re-metamorphosed into high-Fo (94–97) olivines during the second UHP metamorphic epoch (Zhang *et al.* 2008).

Ti-in-zircon thermometry: be careful in the temperature calculation of the low-temperature eclogites

Ti concentrations in zircons have been widely used for metamorphic temperature calculations of rutile-bearing eclogite (e.g. Watson & Harrison 2005; Watson *et al.* 2006). The Ti-in-zircon thermometry reveals that the calculated temperature is positively correlated with the Ti contents in zircons. Using this method, Zhang *et al.* (2014) suggested that the metamorphic temperatures of zircon cores are hotter (*c.* 680°C) than that of zircon rims (*c.* 650°C).

However, we note that the Ti concentrations of zircons show a clear positive correlation with the U content (Fig. 9). Zircons from the lawsonite eclogite have both high Ti and U contents. Using Ti-in-zircon thermometry, the calculated metamorphic temperatures for zircons from the lawsonite eclogite are as

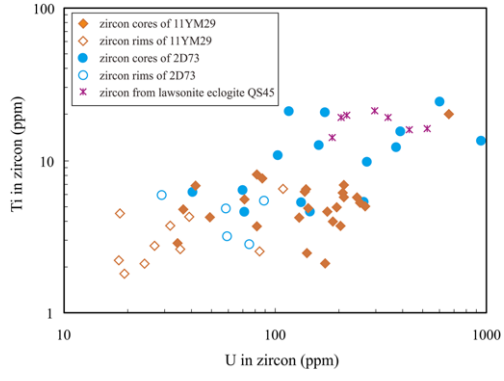

Fig. 9. Diagram of U v. Ti in zircons from eclogites.

high as 850°C, much higher than the temperatures (460–540°C: Song *et al.* 2007; Zhang *et al.* 2007) obtained using the Grt–Cpx Fe–Mg exchange thermometry of Ravna & Terry (2004).

As expected, uranium is a soluble element and its contents can be readily elevated by water-rich fluids during low-temperature, lawsonite eclogite-facies metamorphism. The positive correlation between U and Ti means that the Ti activity in zircons has an unneglectable relationship with water-rich fluids. Therefore, we conclude that the Ti-in-Zircon thermometry is invalid or limited in temperature calculations for low-temperature and fluid-rich eclogites.

Timescale of continental subduction

As described above, eclogites from the ophiolitic sequences have complex, but two distinct, epochs of eclogite-facies metamorphic ages. However, some key rock types, including garnet peridotite, eclogites with CFB protolith, and granitic and pelitic gneisses, that represent the components of continental crust can be used to constrain the timescale of UHP metamorphism related to continental subduction:

- The garnet peridotite, which is only present in UHPM terranes associated with continental-type subduction zones (e.g. Brueckner 1998), recorded UHP metamorphism at depths of *c.* 200 km and gave UHP metamorphic ages of 433–420 Ma (Song *et al.* 2004, 2005; Xiong *et al.* 2011).
- Some eclogites in the North Qaidam UHMP belt have protoliths of CFBs with formation ages ranging from 850 to 820 Ma (e.g. Song *et al.* 2010). They are noted components of the subducted continental crust. These eclogites recorded only a single UHP metamorphic event at *c.* 438–425 Ma (Chen *et al.* 2009; Song *et al.* 2010; J. X. Zhang *et al.* 2010; G. B. Zhang *et al.* 2014).
- Zircons from pelitic and granitic gneisses in the North Qaidam recorded UHP metamorphic ages at 432–423 Ma (Mattinson *et al.* 2006, 2009; Song *et al.* 2006, 2014*a*, *b*; Chen *et al.* 2009).

Therefore, these UHP metamorphic ages recorded by zircons indicate that continent crust might have subducted to a depth of 100 km at *c.* 438 Ma and continued to depths of 200 km at *c.* 433–420 Ma. Assuming that the Qilian Ocean was closed at *c.* 440 Ma and the continents began to subduct with continental collision, the downgoing rate of the continental crust would have been roughly 2–5 cm a^{-1}.

Melting of subducted oceanic crust evoked by hot continental subduction

Generally, the subducted continental crust is composed mostly of felsic gneisses (>80%), buoyant and dry. The protoliths of eclogite are usually continental basalts (e.g. in the North Qaidam UHP belt: Song *et al.* 2010), cumulate gabbros or former high-grade metamorphosed granulite (e.g. Liu *et al.* 2007; Song *et al.* 2012) with an extremely low content of water, and they are difficult to melt during continental subduction and exhumation.

The former subducted oceanic slab is generally cold and wet with water-rich minerals, such as lawsonite, zoisite/epidote and glauscophane. The subsequent continental subduction can disturb the thermal structure of the subduction zone, and part of the subducting oceanic slab will roll back and be accreted to the subduction channel (e.g. Boutelier *et al.* 2004; Beaumont *et al.* 2009; Gerya 2011; Li *et al.* 2011). Therefore, the former cold eclogites will be warmed up with dehydration reactions. When the continental subduction initiated, the former cold slab would be involved in, warmed up and then release water by dehydration of Lws and Ep, and give rise to partial melting by both decompression and water releasing (Song *et al.* 2014*b*) (Fig. 8). This process would, in turn, evoke exhumation of the UHP terrane (e.g. Labrousse *et al.* 2004).

Implications for linking oceanic subduction with continental subduction/collision

The onset of convergence can be constrained by youngest arc volcanic rocks, blueschist and low-temperature eclogites, and remnant sea-basin sediments. Arc volcanic rocks from the North Qilian and Lajishan, as well as low- temperature, HP metamorphism at the Qilian oceanic suture zone, suggest that the Qilian Ocean was finally closed at *c.* 440 Ma (Song *et al.* 2013, 2014*b*), and continental subduction continuously followed the oceanic subduction

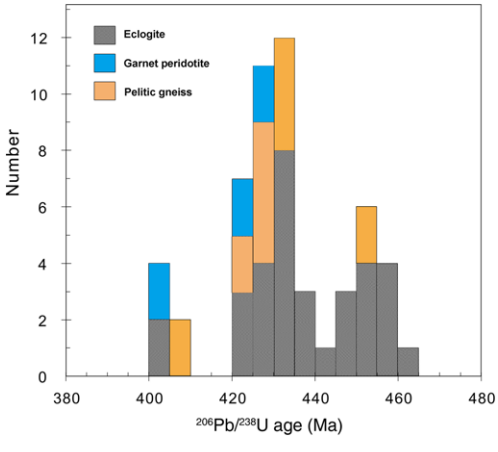

Fig. 10. Distribution of zircon U–Pb ages for various UHPM rocks from the North Qaidam UHPM belt. Data are from Song *et al.* (2014*a*, *b*) and references therein.

and reach depths of 100–200 km at *c.* 438–420 Ma on the basis of metamorphic and geochronological studies of eclogites, garnet peridotite and metapelite (Song *et al.* 2005, 2006, 2014*a*; J. X. Zhang *et al.* 2010; Xiong *et al.* 2011; G. B. Zhang *et al.* 2014). The timescale for the transition from oceanic subduction to continental collision and then subduction to depths *c.* 100 km is about 7 myr.

The distribution of all reliable zircon U–Pb ages for various UHPM rocks from the North Qaidam UHPM belt (Fig. 10) illustrates the two major epochs of metamorphism, except for the late (<420 Ma) retrograde overprinting. The gap in-between 445 and 440 Ma, with only one age presented, further suggested a transition from the end of oceanic subduction and continental colliding initiation at *c.* 445 Ma, to continental deep subduction with UHP metamorphism at *c.* 438–420 Ma.

Our study provides evidence for two epochs of eclogite-facies metamorphism in individual eclogite samples in the North Qaidam UHP belt, which recorded a complex, but a complete, cycle from oceanic 'cold' subduction to continental 'warm' subduction over a timescale of *c.* 40 myr. Such a cycle may represent the transition of subduction channel dynamics from Franciscan-type (or oceanic-type) (e.g. Gerya *et al.* 2002; Agard *et al.* 2009) to Alpine-type (or continental-type) (Ernst 2001; Song *et al.* 2006). In any case, the remarkable two epochs of eclogite-facies metamorphism present a better understanding of the links between the oceanic subduction and the following continental collision and subduction.

Acknowledgements We thank the editor and two reviewers for their constructive comments and suggestions to this manuscript.

Funding This study was supported by the Major State Basic Research Development Program (grant No. 2015CB856105 to S. Song) and the National Natural Science Foundation of China (funding agency ID: doi.org/10.13039/501100001809; grant Nos 41372060 and 41572040 to S. Song).

References

Agard, P., Yamato, P., Jolivet, L. & Burov, E. 2009. Exhumation of oceanic blueschists and eclogites in subduction zones: timing and mechanisms. *Earth-Science Reviews*, **92**, 53–79.

Beaumont, C., Jamieson, R.A., Butler, J.P. & Warren, C. J. 2009. Crustal structure: a key constraint on the mechanism of ultrahigh-pressure rock exhumation. *Earth and Planetary Science Letters*, **287**, 116–129.

Black, L.P., Kamo, S.L., Allen, C.M., Aleinikoff, J.N., Davis, D.W., Korsch, R.J. & Foudoulis, C. 2003. TEMORA 1: a new zircon standard for Phanerozoic U–Pb geochronology. *Chemical Geology*, **200**, 155–170.

Boutelier, D., Chemenda, A. & Jorand, C. 2004. Continental subduction and exhumation of high-pressure rocks: insights from thermo-mechanical laboratory modelling. *Earth and Planetary Science Letters*, **222**, 209–216.

Brueckner, H.K. 1998. Sinking intrusion model from the emplacement of garnet-bearing peridotites into continent collision orogens. *Geology*, **26**, 631–634.

Brueckner, H.K. 2006. Dunk, dunkless and re-dunk tectonics: a model for metamorphism, lack of metamorphism, and repeated metamorphism of HP/UHP terranes. *International Geology Review*, **48**, 978–995.

Brueckner, H.K. 2011. Geodynamics: double-dunk tectonics. *Nature Geoscience*, **4**, 136–138.

Carswell, D.A. 1990. *Eclogite Facies Rocks*. Blackie, Glasgow.

Chemenda, A.I., Mattauer, M. & Bokun, A.N. 1996. Continental subduction and a mechanism for exhumation of high-pressure metamorphic rocks: new modelling and field data from Oman. *Earth and Planetary Science Letters*, **143**, 173–182.

Chen, D.L., Liu, L., Sun, Y. & Liou, J.G. 2009. Geochemistry and zircon U–Pb dating and its implications of the Yukahe HP/UHP terrane, the North Qaidam, NW China. *Journal of Asian Earth Sciences*, **35**, 259–272.

Clarke, G.L., Aitchison, J.C. & Cluzel, D. 1997. Eclogites and blueschists of the Pam Peninsula, NE New Caledonia: a reappraisal. *Journal of Petrology*, **38**, 843–876.

Compston, W., Williams, I.S., Kirschvink, J.L., Zhang, Z. & Ma, G. 1992. Zircon U–Pb ages for the Early Cambrian time-scale. *Journal of the Geological Society, London*, **149**, 171–184, https://doi.org/10.1144/gsjgs.149.2.0171

Droop, G.R.T. 1987. A general equation for estimating Fe^{3+} microprobe analyses, using stoichiometric criteria. *Mineralogical Magazine*, **51**, 431–435.

Ernst, W.G. 2001. Subduction, ultrahigh-pressure metamorphism, and regurgitation of buoyant crustal slices – implications for arcs and continental growth. *Physics of the Earth and Planetary Interiors*, **127**, 253–275.

Ernst, W.G. 2005. Alpine and Pacific styles of Phanerozoic mountain building: subduction-zone petrogenesis of continental crust. *Terra Nova*, **17**, 165–188.

Gerya, T. 2011. Future directions in subduction modeling. *Journal of Geodynamics*, **52**, 344–378.

Gerya, T., Stockhert, B. & Perchuk, A. 2002. Exhumation of high-pressure metamorphic rocks in a subduction channel: a numerical simulation. *Tectonics*, **21**, T1056.

Han, L. 2015. *Petrology study of Yematan eclogite from North Qaidam, China*. PhD thesis, Peking University.

Herwartz, D., Nagel, T.J., Munker, C., Scherer, E.E. & Froitzheim, N. 2011. Tracing two orogenic cycles in one eclogite sample by Lu–Hf garnet chronometry. *Nature Geoscience*, **4**, 178–183.

Labrousse, L., Jolivet, L., Andersen, T.B., Agard, P., Hébert, R., Maluski, H. & Schärer, U. 2004. Pressure–temperature–time deformation history of the exhumation of ultra-high pressure rocks in the Western Gneiss Region, Norway. *In*: Whitney, D.L., Teyssier, C. & Siddoway, C.S. (eds) *Gneiss Domes in Orogeny*. Geological Society of America, Special Papers, **380**, 155–183.

LI, Z.H., XU, Z.Q. & GERYA, T.V. 2011. Flat v. steep subduction: contrasting modes for the formation and exhumation of high- to ultrahigh-pressure rocks in continental collision zones. *Earth and Planetary Science Letters*, **301**, 65–77.

LIU, X.C., WU, Y.B. *ET AL.* 2012. First record and timing of UHP metamorphism from zircon in the Xitieshan terrane: implications for the evolution of the entire North Qaidam metamorphic belt. *American Mineralogist*, **97**, 1083–1093.

LIU, Y.C., LI, S.G., GU, X.F., XU, S.T. & CHEN, G.B. 2007. Ultrahigh-pressure eclogite transformed from mafic granulite in the Dabie orogen, east-central China. *Journal of Metamorphic Geology*, **25**, 975–989.

LUDWIG, K.R. 2003. *User's manual for isoplot 3.00: a geochronological toolkit for Microsoft Excel*. Special Publication Berkeley Geochronology Centre, **4**. Berkeley, California.

MARUYAMA, S., LIOU, J.G. & TERABAYASHI, M. 1996. Blueschists and eclogites of the world and their exhumation. *International Geology Review*, **38**, 485–594.

MATTINSON, C.G., WOODEN, J.L., LIOU, J.G., BIRD, D.K. & WU, C.L. 2006. Age and duration of eclogite-facies metamorphism, North Qaidam HP/UHP terrane, western China. *American Journal of Science*, **306**, 683–711.

MATTINSON, C.G., WOODEN, J.L., ZHANG, J. & BIRD, D.K. 2009. Paragneiss zircon geochronology and trace element geochemistry, North Qaidam HP/UHP terrane, western China. *Journal of Asian Earth Sciences*, **35**, 298–309.

PEACOCK, S.M. & WANG, K. 1999. Seismic consequences of warm v. cool subduction metamorphism: examples from southwest and northeast Japan. *Science*, **286**, 937–939.

PEARCE, N.J.G., PERKINS, W.T., WESTGATE, J.A., GORTON, M.P., JACKSON, S.E., NEAL, C.R. & CHENERY, S.P. 1997. A compilation of new and published major and trace element data for NIST SRM 610 and NIST SRM 612 glass reference materials. *Geostandards Newsletter*, **21**, 115–144.

POLI, S. & SCHMIDT, M.W. 2002. Petrology of subducted slabs. *Annual Review of Earth and Planetary Sciences*, **30**, 207–235.

RAVNA, E.J.K. & TERRY, M.P. 2004. Geothermobarometry of UHP and HP eclogites and schists – an evaluation of equilibria among garnet–clinopyroxene–kyanite–phengite–coesite/quartz. *Journal of Metamorphic Geology*, **22**, 579–592.

RUBATTO, D., REGIS, D., HERMANN, J., BOSTON, K., ENGI, M., BELTRANDO, M. & MCALPINE, S.R.B. 2011. Yo-yo subduction recorded by accessory minerals in the Italian Western Alps. *Nature Geoscience*, **4**, 338–342.

SONG, S.G., YANG, J.S., LIOU, J.G., WU, C.L., SHI, R.D. & XU, Z.Q. 2003*a*. Petrology, Geochemistry and isotopic ages of eclogites in the Dulan UHPM terrane, the North Qaidam, NW China. *Lithos*, **70**, 195–211.

SONG, S.G., YANG, J.S., XU, Z.Q., LIOU, J.G., WU, C.L. & SHI, R.D. 2003*b*. Metamorphic evolution of coesite-bearing UHP terrane in the North Qaidam, northern Tibet, NW China. *Journal of Metamorphic Geology*, **21**, 631–644.

SONG, S.G., ZHANG, L.F. & NIU, Y. 2004. Ultra-deep origin of garnet peridotite from the North Qaidam ultrahigh-pressure belt, Northern Tibetan Plateau, NW China. *American Mineralogist*, **89**, 1330–1336.

SONG, S.G., ZHANG, L.F., NIU, Y.L., SU, L., JIAN, P. & LIU, D.Y. 2005. Geochronology of diamond-bearing zircons from garnet peridotite in the North Qaidam UHPM belt, Northern Tibetan Plateau: a record of complex histories from oceanic lithosphere subduction to continental collision. *Earth and Planetary Science Letters*, **234**, 99–118.

SONG, S.G., ZHANG, L.F., NIU, Y.L., SU, L., SONG, B. & LIU, D.Y. 2006. Evolution from oceanic subduction to continental collision: a case study from the Northern Tibetan Plateau Based on geochemical and geochronological data. *Journal of Petrology*, **47**, 435–455.

SONG, S.G., ZHANG, L.F., NIU, Y.L., WIE, C.J., LIOU, J.G. & SHU, G.M. 2007. Eclogite and carpholite-bearing metasedimentary rocks in the North Qilian suture zone, NW China: implications for early Palaeozoic cold oceanic subduction and water transport into mantle. *Journal of Metamorphic Geology*, **25**, 547–563.

SONG, S.G., SU, L., NIU, Y.L., ZHANG, G.B. & ZHANG, L.F. 2009. Two types of peridotite in North Qaidam UHPM belt and their tectonic implications for oceanic and continental subduction: a review. *Journal of Asian Earth Sciences*, **35**, 285–297.

SONG, S.G., SU, L., LI, X.-h., ZHANG, G.B., NIU, Y.L. & ZHANG, L.F. 2010. Tracing the 850-Ma continental flood basalts from a piece of subducted continental crust in the North Qaidam UHPM belt, NW China. *Precambrian Research*, **183**, 805–816.

SONG, S.G., SU, L., LI, X.H., NIU, Y.L. & ZHANG, L.F. 2012. Grenville-age orogenesis in the Qaidam-Qilian block: the link between South China and Tarim. *Precambrian Research*, **220**, 9–22.

SONG, S.G., NIU, Y.L., SU, L. & XIA, X.H. 2013. Tectonics of the North Qilian orogen, NW China. *Gondwana Research*, **23**, 1378–1401.

SONG, S.G., NIU, Y.L., SU, L., WEI, C.J. & ZHANG, L.F. 2014*a*. Adakitic tonalitic–trondhjemitic magmas resulting from eclogite decompression and dehydration melting during exhumation in response to continental collision. *Geochimica et Cosmochimica Acta*, **130**, 42–62.

SONG, S.G., NIU, Y.L., SU, L., ZHANG, C. & ZHANG, L.F. 2014*b*. Continental orogenesis from ocean subduction, continent collision/subduction, to orogen collapse, and orogen recycling: the example of the North Qaidam UHPM belt, NW China. *Earth-Science Reviews*, **129**, 59–84.

STACEY, J.S. & KRAMERS, J.D. 1975. Approximation of terrestrial lead isotope evolution by a two-stage model. *Earth and Planetary Science Letters*, **26**, 207–221.

WATSON, E.B. & HARRISON, T.M. 2005. Zircon thermometer reveals minimum melting conditions on earliest Earth. *Science*, **308**, 841–844.

WATSON, E.B., WARK, D. & THOMAS, J. 2006. Crystallization thermometers for zircon and rutile. *Contributions to Mineralogy and Petrology*, **151**, 413–433.

WEI, C.J., YANG, Y., SU, X.L. & SONG, S.G. 2009. Metamorphic evolution of low-T eclogite from the North Qilian orogen, NW China: evidence from petrology and calculated phase equilibria in the system NCKFMASHO. *Journal of Metamorphic Geology*, **27**, 55–70.

WHITNEY, D.L. & DAVIS, P.B. 2006. Why is lawsonite eclogite so rare? Metamorphism and preservation of

lawsonite eclogite, Sivrihisar, Turkey. *Geology*, **34**, 473–476.

Whitney, D.L. & Evans, B.W. 2010. Abbreviations for names of rock-forming minerals. *American Mineralogist*, **95**, 185–187.

Xiao, Y.Y., Lavis, S., Niu, Y.L., Pearce, J.A., Li, H.K., Wang, H.C. & Davidson, J. 2012. Trace element transport during subduction-zone ultrahigh pressure metamorphism: evidence from Western Tianshan, China. *Geological Society of America Bulletin*, **124**, 1113–1129.

Xiao, Y.Y., Niu, Y.L., Song, S.G., Davidson, J. & Liu, X. M. 2013. Elemental responses to subduction-zone metamorphism: constraints from the North Qilian Mountain, NW China. *Lithos*, **160–161**, 55–67.

Xiong, Q., Zheng, J., Griffin, W.L., O'Reilly, S.Y. & Zhao, J. 2011. Zircons in the Shenglikou ultrahigh-pressure garnet peridotite massif and its country rocks from the North Qaidam terrane western China: Meso-Neoproterozoic crust–mantle coupling and early Paleozoic convergent plate-margin processes. *Precambrian Research*, **187**, 33–57.

Xu, X., Song, S., Allen, M.B., Ernst, R.E., Niu, Y. & Su, L. 2016. An 850–820 Ma LIP dismembered during breakup of the Rodinia supercontinent and destroyed by Early Paleozoic continental subduction in the northern Tibetan Plateau, NW China. *Precambrian Research*, **282**, 52–73.

Yang, J.S., Xu, Z.Q. *et al.* 2002. Subduction of continental crust in the early Palaeozoic North Qaidam ultrahigh-pressure metamorphic belt, NW China: evidence from the discovery of coesite in the belt. *Acta Geologica Sinica – English Edition*, **76**, 63–68.

Zhang, G.B., Song, S.G., Zhang, L.F. & Niu, Y.L. 2008. The subducted oceanic crust within continental-type UHP metamorphic belt in the North Qaidam, NW China: evidence from petrology, geochemistry and geochronology. *Lithos*, **104**, 99–118.

Zhang, G.B., Zhang, L.F. & Song, S.G. 2009. UHP metamorphic evolution and SHRIMP geochronology of a metaophiolitic gabbro in the North Qaidam, NW China. *Journal of Asian Earth Sciences*, **35**, 310–322.

Zhang, G.B., Zhang, L.F., Christy, A.G., Song, S.G. & Li, Q.L. 2014. Differential exhumation and cooling history of North Qaidam UHP metamorphic rocks, NW China: constraints from zircon and rutile thermometry and U–Pb geochronology. *Lithos*, **205**, 15–27.

Zhang, J.X., Meng, F.C. & Wan, Y.S. 2007. A cold Early Palaeozoic subduction zone in the North Qilian Mountains, NW China: petrological and U–Pb geochronological constraints. *Journal of Metamorphic Geology*, **25**, 285–304.

Zhang, J.X., Mattinson, C.G., Yu, S.Y., Li, J.P. & Meng, F.C. 2010. U–Pb zircon geochronology of coesite-bearing eclogites from the southern Dulan area of the North Qaidam UHP terrane, northwestern China: spatially and temporally extensive UHP metamorphism during continental subduction. *Journal of Metamorphic Geology*, **28**, 955–978.